ORGANIC CHEMISTRY
FRONTIERS

RESEARCH ARTICLE

View Article Online
View Journal

Cite this: DOI: 10.1039/d5qo01537e

Visible-light-driven C–H functionalization of double bonds with diazo compounds under mild reaction conditions

Miguel A. Valle-Amores,[a] Benedetta Carli,[a] Ian MacLean,[a] Lara Martínez-Fernández,[b] Raúl Pérez-Ruíz,[c] Leyre Marzo,*[a,d] Alberto Fraile*[a,d] and José Alemán*[a,d]

Received 7th November 2025,
Accepted 17th March 2026

DOI: 10.1039/d5qo01537e

rsc.li/frontiers-organic

Expanding the toolbox of C–H functionalization reactions applicable to the late-stage modification of complex molecules of interest in medicinal chemistry is a key strategy for drug development. Herein, we report an unusual visible-light-induced olefinic C(sp^2)–H functionalization of olefins with diazo derivatives using an Ir(III) photocatalyst. The approach demonstrates the potential for targeting double bonds, such as those present in enol ethers, and has been further applied to 1,1-disubstituted alkenes. This efficient methodology affords unprecedented Heck-type products in good to excellent yields under mild conditions. Further derivatizations of the final products are shown to demonstrate the robustness of the methodology. The reaction pathway was validated through electrochemical and photophysical experiments as well as computational studies.

Introduction

Diazo compounds are widely used in organic chemistry as synthetic building blocks in numerous reactions due to their high reactivity and straightforward integration into numerous chemical transformations under mild conditions, which allow diverse applications.[1] These nitrogenated structures are considered as environmentally benign alkylation reagents, featuring the advantage of N_2 as a leaving group and the sole byproduct under neutral conditions. From a synthetic point of view, diazo compounds can be considered as carbene synthetic equivalents and their reactivity has been exploited in many applications ranging from cycloaddition,[2] rearrangement,[2e,3] insertion,[4] ylide formation,[5] cross-coupling,[6] and C–H functionalization reactions.[7] Traditionally, transition metal catalysts were commonly employed to control and access the reactivity of carbene intermediates.[8] Nevertheless, during the last decades, UV/visible light-mediated strategies have emerged as a key useful tool for the direct activation of diazo compounds (right, Scheme 1a). In this context, pioneering work reported by Jurberg and Davies in 2018,[9a] disclosed that aryl diazoacetates could absorb visible light, leading to the generation of singlet carbene species *via* direct photolysis.[9] This work opened the door to many applications, leading to improvements to existing reactions. In this regard, in 2019, a catalyst-free cyclopropanation reaction of donor/acceptor diazo compounds and alkynes under blue LED irradiation (470 nm) was described in a very operationally simple protocol (Scheme 1b).[10] However, direct photolysis of diazo compounds has the intrinsic limitation of being dependent on the photochemical properties of each diazo derivative, and in this sense, its application is limited to donor/acceptor (able to absorb visible light irradiation from 400 to 500 nm) and donor/donor diazo compounds (400 to 600 nm) (see bottom of Scheme 1a).[11] To broaden the scope and overcome these limitations, photocatalysis has emerged as a powerful synthetic tool (left, Scheme 1a).[12] On the one hand, diazo compounds can be activated *via* energy transfer (EnT) to form triplet carbenes, enabling the use of diazo compounds that do not absorb visible light.[13] Thus, this method was used for *gem*-difluoroolefination of α-trifluoromethyl(styrene) with diazoacetates, where DABCO promoted a [2 + 1] cycloaddition between carbene and double bonds.[13b] In addition, the photochemically generated carbene was successfully stabilized by trapping it with a cobalt complex.[14] On the other hand, the reduction of diazo compounds can facilitate the formation of carbon-centered radicals.

---

[a] *Departamento de Química Orgánica (Módulo 1), Universidad Autónoma de Madrid, Calle Francisco Tomás y Valiente 7, Madrid, 28049, Spain. E-mail: leyre.marzo@uam.es, alberto.fraile@uam.es, jose.aleman@uam.es*
[b] *Instituto de Química Física Blas Cabrera, Consejo Superior de Investigaciones Científicas, Calle Serrano 119, Madrid, 28006, Spain*
[c] *Departamento de Química, Universitat Politècnica de València, Camino de Vera S/N, Valencia, 46022, Spain*
[d] *Institute for Advanced Research in Chemical Sciences (IAdChem), Universidad Autónoma de Madrid, Calle Francisco Tomás y Valiente 7, Madrid, 28049, Spain*

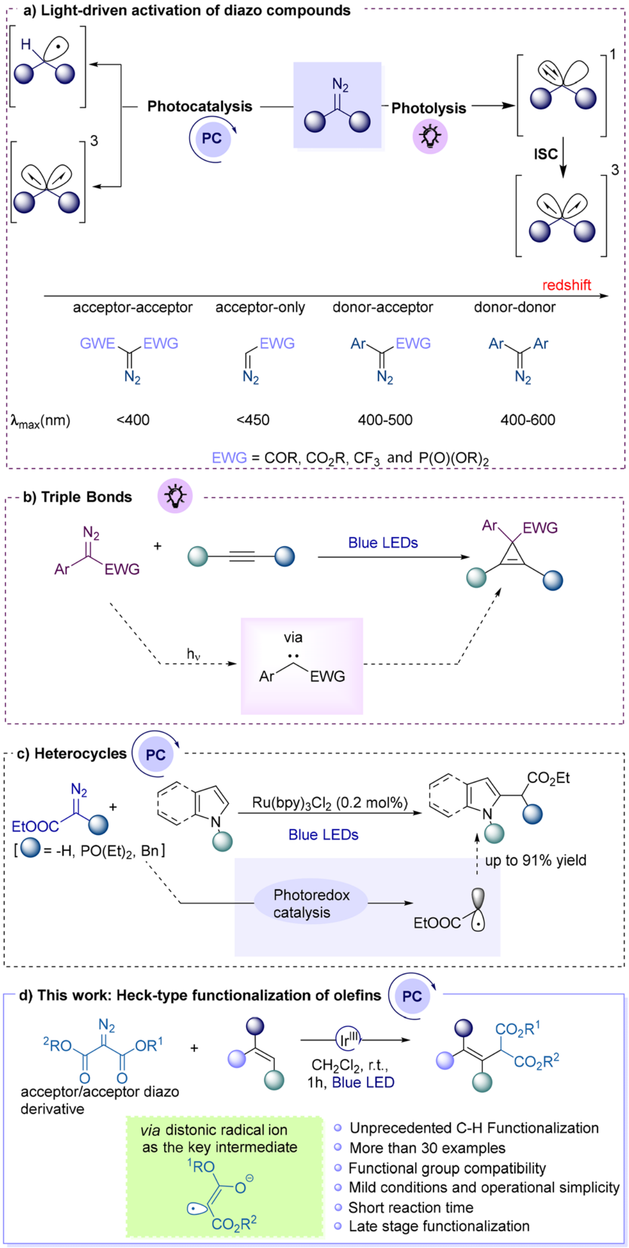

Scheme 1 Background and synopsis of the present work. (a) Light-driven activation of diazo compounds. (b) Cyclopropanation reaction. (c) Radical-mediated strategy. (d) This work: photocatalytic C–H functionalization of double bonds.

This activation may be accomplished through a proton coupled electron transfer process (PCET)[15] or by direct reduction *via* a single electron transfer (SET) event,[16] in which the generation of carbon-centred radicals is achieved through the direct reduction of acceptor-type diazo compounds (Scheme 1c).[16a] These radicals are subsequently added to electron-rich heteroarenes, thus establishing a novel photocatalytic method for the alkylation of indoles and pyrroles.

This method, while effective, is restricted to acceptor-only diazoalkanes. Alternatively, the reaction of acceptor/acceptor diazoalkanes under photochemical conditions remains largely underexplored. Considering all this background, the lack of examples in the literature of C–H functionalization of olefins with diazoalkanes, and the use of acceptor/acceptor diazo compounds, we envisioned a mild strategy for the C(sp^2)–H functionalization of olefins using diazomalonates as carbon-centered radical precursors under visible-light irradiation and an external photocatalyst. Furthermore, the installation of malonate esters is very valuable owing to the number of possible further transformations that can be conducted using this functional group, such as the malonic ester synthesis to furnish substituted acid derivatives.[17] Herein, we report our studies of acceptor/acceptor diazo compounds to functionalize a wide variety of olefins, achieving Heck-type products in good yields and excellent group tolerance under mild reaction conditions (Scheme 1d). This approach will avoid the formation of cyclopropane derivatives, which are the main products obtained when diazo compounds react with alkenes under light.[18] A plausible distonic radical anion[19] is the key intermediate in the reduction of diazo derivatives. Due to the simple and mild reaction conditions and short reaction times (1–3 h), this methodology could be further applied in the modification of complex molecules of interest in drug discovery.

Results and discussion

Our investigation began by selecting the non-visible-light-absorbing diazomalonate **1a** and the electron-rich olefin **2a** (TBDMS was selected as a protecting group due to its higher stability under silica gel) as model substrates (Table 1). *Fac*-Ir(ppy)$_3$ was used as the photocatalyst at room temperature, under blue LED irradiation (460 nm) and a nitrogen atmosphere. The reaction mixture was stirred for 16 hours in dichloromethane. Gratifyingly, the desired product **3aa** was afforded in 40% ^{1}H NMR yield as a mixture of isomers ($E:Z$ = 40 : 60) (entry 1, Table 1).

Encouraged by this result, more equivalents of **2a** were tested (entries 2 and 3), which improved the reaction efficiency to 86% ^{1}HNMR yield. Control experiments confirmed that light and a photocatalyst were indispensable in this process (entries 4 and 5). The kinetics of the reaction (Fig. S8) showed an excellent 87% ^{1}HNMR yield in just 1 h of reaction time, which was further used as the optimal time in the subsequent studies (entry 6). We next investigated the influence of the photocatalyst, with *fac*-Ir(ppy)$_3$ identified as the optimal candidate for this purpose since other photocatalysts showed lower efficiency or no product formation (entries 7–11 and Table S1). Surprisingly, when the reaction was tested without a N_2 atmosphere, results similar to those obtained under an inert atmosphere (entry 12) were achieved. Further optimization was conducted by screening a variety of reaction solvents such as 1,2-dichloroethane, chloroform, acetonitrile and methanol, and even under neat conditions, but they all provided unsatisfactory results except for 1,2-DCE, which enabled the formation of **3aa** in a slightly decreased yield (entries 13–15 and

Table 1 Optimization of the reaction conditions[a]

Entry	Ratio (**1a** : **2a**)	Solvent	Photocatalyst (mol%)	Time (h)	Yield[b] (%)
1[c]	1 : 2	CH_2Cl_2	*fac*-Ir(ppy)$_3$ (5)	16	40
2[c]	1 : 3	CH_2Cl_2	*fac*-Ir(ppy)$_3$ (5)	16	56
3[c]	1 : 4	CH_2Cl_2	*fac*-Ir(ppy)$_3$ (5)	16	86
4[c]	1 : 4	CH_2Cl_2	—	16	nr
5[c,d]	1 : 4	CH_2Cl_2	*fac*-Ir(ppy)$_3$ (5)	16	nr
6[c]	1 : 4	CH_2Cl_2	*fac*-Ir(ppy)$_3$ (5)	1	87
7[c]	1 : 4	CH_2Cl_2	[Ir{dF[CF$_3$(ppy)$_2$(dtbpy)]}] PF$_6$ (5)	1	71
8[c]	1 : 4	CH_2Cl_2	[Ir(dF-ppy)$_3$] PF$_6$ (5)	1	68
9[c]	1 : 4	CH_2Cl_2	[Ru(bpy)$_3$] Cl$_2$ (5)	1	nr
10[c]	1 : 4	CH_2Cl_2	4CzIPN (5)	1	nr
11[c]	1 : 4	CH_2Cl_2	[Ir(ppy)$_2$(dtbpy)] PF$_6$ (5)	1	20
12	1 : 4	CH_2Cl_2	*fac*-Ir(ppy)$_3$ (5)	1	87
13	1 : 4	DCE	*fac*-Ir(ppy)$_3$ (5)	1	83
14	1 : 4	MeCN	*fac*-Ir(ppy)$_3$ (5)	1	nr
15	1 : 4	MeOH	*fac*-Ir(ppy)$_3$ (5)	1	nr
16[e]	1 : 4	CH_2Cl_2	*fac*-Ir(ppy)$_3$ (5)	1	62
17	1 : 4	CH_2Cl_2	*fac*-Ir(ppy)$_3$ (2.5)	1	51
18	1 : 4	CH_2Cl_2	*fac*-Ir(ppy)$_3$ (1)	1	27

[a] Reaction conditions: a mixture of **1a** (1.0 equiv., 0.1 mmol), **2a** (indicated equiv.), and the indicated photocatalyst (0.1 mol%) in the indicated solvent (0.1 M) was irradiated with blue LED in air at 25 °C for the indicated time, unless otherwise noted. The wavy bond indicates that the product was isolated as a mixture of *Z* and *E* diastereoisomers. nr = no reaction. [b] Determined by ^1H NMR analysis using 1,3,5-trimethoxybenzene as the internal standard. [c] Under a N_2 atmosphere. [d] No light was used in this case. [e] In this case, 0.2 M was used.

Table S2). Importantly, modification of reaction concentrations had a remarkable effect on the yields. Thus, increasing (0.2 M) or decreasing (0.05 M) the concentration did not improve the result obtained when 0.1 M was used, the latter being the optimal. Finally, attempts to decrease the catalyst loading led to the formation of the Heck-type product **3aa** in lower yields (entries 17 and 18). It should be noted that the *E*/*Z* ratio (*E* : *Z* = 40 : 60) was maintained almost unaltered for all assays.

Having addressed the optimal conditions for this transformation (entry 12, Table 1), we next explored the substrate scope and limitations of the process (Scheme 2). First, variations in the structure of the diazo compounds under the optimized conditions showed that methyl 2-diazo-2-(diethoxyphosphoryl)acetate (**1b**) and di-*tert*-butyl 2-diazomalonate (**1c**) were fully compatible with the present protocol affording products **3ba** and **3ca** in useful yields. Other types of diazo compounds with different electron-withdrawing groups (EWGs) (ketones and amides) were also tested and found to be ineffective for the C–H functionalization, providing a high dependency on the diazo pattern. Then, we studied the reaction with different double bonds.

The introduction of halogens at *ortho*-, *meta*- and *para*-positions at the aromatic ring provided the corresponding products in good to excellent yields (**3ab–3ae**, 71–93% yields), representing an advantage compared to other works,[14] in which dehalogenation products were observed. *Para*- and *meta*-EDGs such as methyl (**2f** and **2g**) or methoxy (**2h**) were also compatible with the system, allowing the formation of **3af–3ah** in moderate yields (36–54% yields). Moreover, electron-withdrawing groups at the *para*-position were also tested, affording better results when introducing a *para*-CF$_3$ (**3ai**, 79% yield) than a *para*-CN group at the aromatic ring (**3aj**, 64% yield). To our delight, the evaluation of pyridine (**2k**), pyrazine (**2l**) and naphthalene (**2m**) derivatives yielded the final products **3ak–3am** in good to very good yields (56–82% yield). Interestingly, **3al** could be obtained on a larger scale (1.0 mmol) with a slight decrease in the yield. Additionally, the introduction of α-substituents in the double bond, such as methyl (**2n**), ethyl (**2o**) and phenyl (**2p**) groups, furnished C–H functionalized products (**3an–3ap**, 52–62% yields) in moderate to good yields. As expected, aliphatic cyclic structures such as the 5-membered ring (**2q**), the 6-membered ring (**2r**) and the tetralone derivative (**2s**) showed great compatibility with the system, yielding **3aq–3as** in very good yields (66–73% yields). Finally, to show the robustness of this novel methodology, a hormone derivative from estrone (**2t**) was tested under our reaction conditions. To our delight, the desired C–H functionalized product **3at** was smoothly afforded in a useful 43% yield. Although it may initially seem like a disadvantage, the formation of these *Z*–*E* mixtures in the enolate does not influence the final outcome after functionalization or synthetic transformations (see below).

Once the scope of silyl enol ethers was evaluated for this C–H functionalization (Scheme 2), we sought to apply and expand our methodology for the malonate functionalization of different double bonds, highlighting the usefulness of the C–H functionalization of olefins. In this regard, we envisioned the application of the same photocatalytic system to diarylethene derivatives **4** (Scheme 3). As a starting point, symmetric 1,1-diphenylethylene (**4a**) was subjected to the optimized conditions (entry 12, Table 1), affording Heck-type **5aa** as the sole product in 70% yield (Scheme 3). The introduction of symmetric electron-donating groups at the *para*-position such as methyl (**4b**), methoxy (**4c**) and dimethylamine (**4d**) derivatives gave access to the C–H functionalized products in moderate to excellent yields (**5ab–5ad**, 33–93% yields), while the introduction of halogens at the *para*-position such as fluorine (**4e**) afforded the final functionalized product **5ae**.

Next, we envisioned the C–H functionalization of relevant molecules with our photocatalytic approach, such as 9-methylene-9*H*-thioxanthene (**4f**) and 9-methylene-9*H*-xanthene (**4g**), which afforded the corresponding functionalized adducts in very good yields (**5af** and **5ag** in 82 and 67% yields, respectively). Furthermore, attempts to expand the scope of the olefins using unsymmetrical double bonds were found to be critical. In this sense, unsymmetrical 1-methoxy-4-(1-phenylvinyl)benzene (**4h**) was tested under the photocatalytic reaction conditions obtaining the final product **5ah** in 47% yield. However, unsymmetrical double bonds such as those present in 1-methoxy-2-(1-phenylvinyl)benzene (**4i**) and 1-bromo-4-(1-

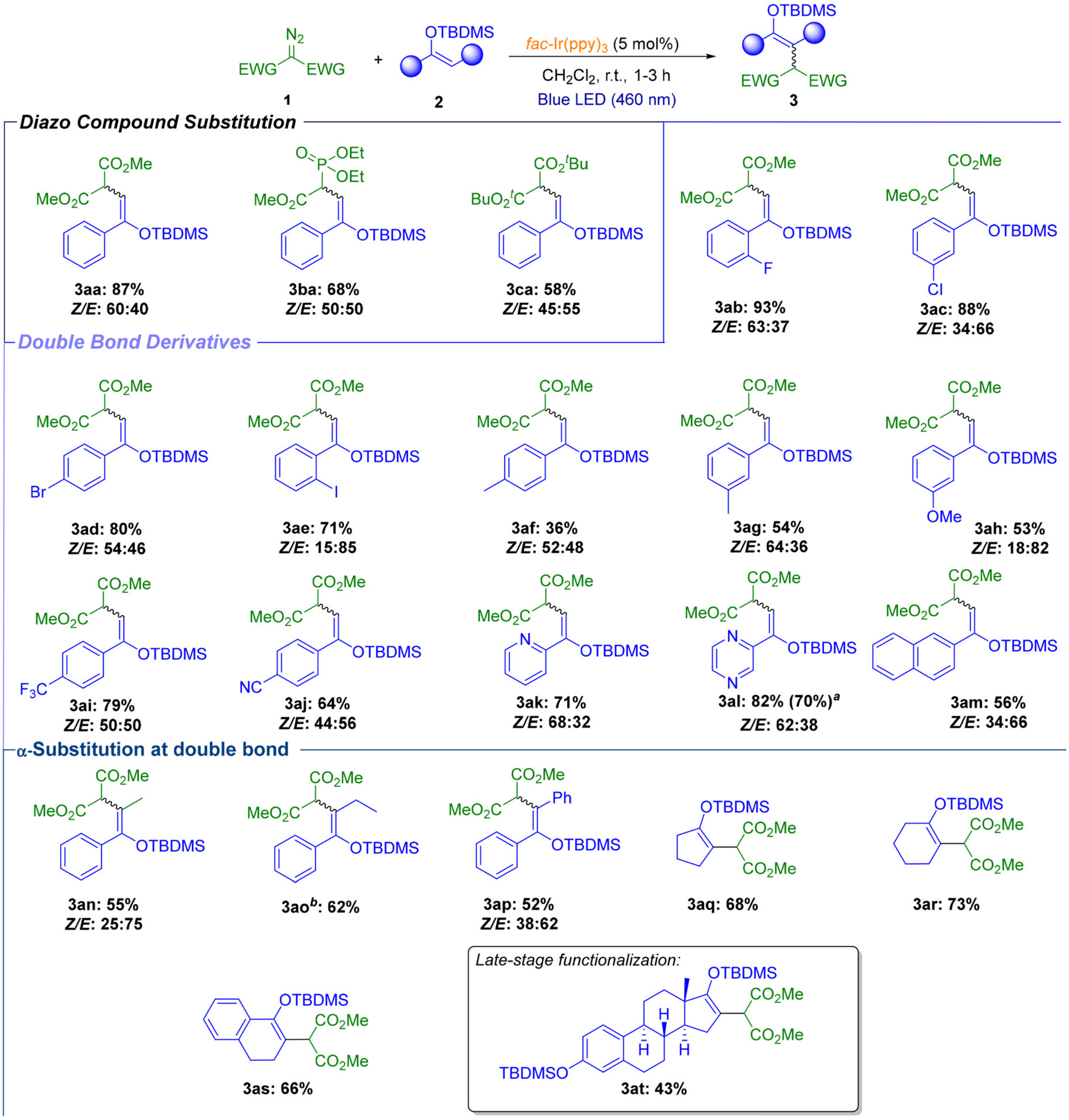

Scheme 2 Reaction scope with silyl enol ethers **2**. Reaction conditions: **1** (0.1 mmol), **2** (4 equiv.) *fac*-Ir(ppy)$_3$ (5 mol%), CH_2Cl_2 (1 mL), and blue LED in air. Isolated yield after flash column chromatography. The wavy bond indicates that the product was isolated as a mixture of *Z* and *E* diastereoisomers (see the SI for details). ^{a} Between parentheses, the yield was obtained when the reaction was carried out on a larger scale using 1.0 mmol of **1a** and 4.0 mmol of **2l**. ^{b} Isolated as the corresponding ketone after reaction with TBAF (2 equiv.), see the SI.

phenylvinyl)benzene (**4j**) gave access to the formation of the corresponding adducts in moderate yields (**5ai** and **5aj** in 9 and 12% yields, respectively), since the formation of the cyclopropanated adducts in these cases was observed (**6ai** and **6aj** in 62 and 69% yields, see section 6.3 in the SI). In addition to the last results obtained, we also carried out the photocatalytic reaction with 1-alkyl-1-phenylstyrenes and monosubstituted styrene derivatives, obtaining the corresponding cyclopropane as the only product (see section 6.3 in the SI). On the other hand, the reaction with alkenes bearing alkyl substituents, such as cyclohexane and dicyclohexylethylene, only afforded a complex mixture. These results highlight the dependency of the C–H functionalization process not only on the diazo pattern but also on the electronic nature and the steric group hindrance of the double bond.

Moreover, to showcase the utility and practicability of the developed process, further applications of product **3aa** were conducted (Scheme 4). First, the Mukaiyama aldol addition to benzaldehyde successfully yielded the corresponding aldol product (**7aa**) in a useful 50% yield (Scheme 4a). In addition, the α-pyrazole ketone derivative (**8aa**) was obtained through CAN oxidative heteroarylation in good yield (70%). On the

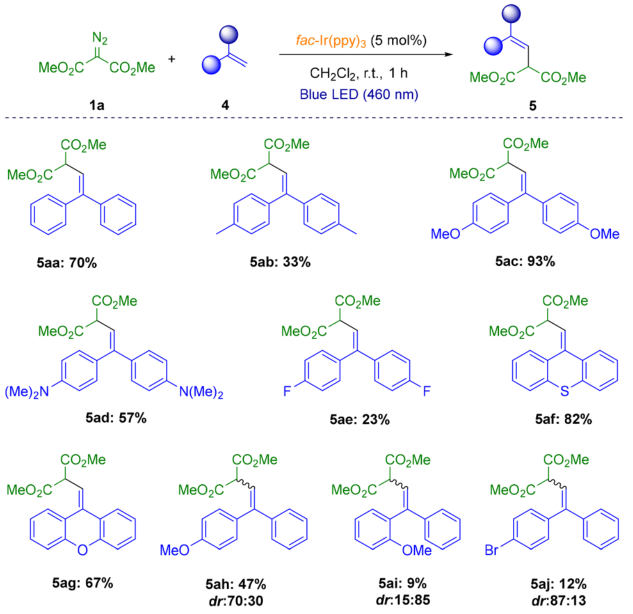

Scheme 3 Reaction Scope with 1,1-disubstituted alkenes **3**. Reaction conditions: **1** (0.1 mmol), **2** (4 equiv.), *fac*-Ir(ppy)$_3$ (5 mol%), CH$_2$Cl$_2$ (1 mL), blue LED in air, 1 h. Isolated yield after flash column chromatography.

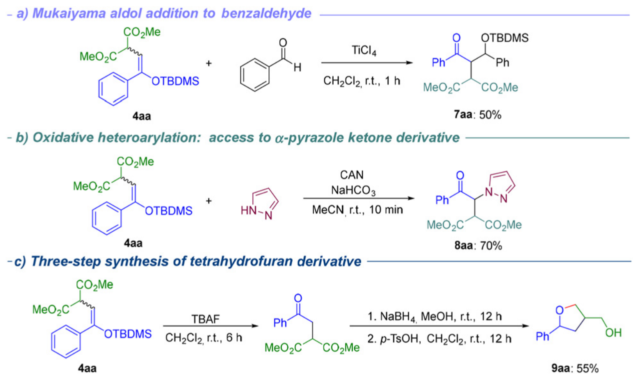

Scheme 4 Further applications of the Heck-type products **3aa**. (a) Mukaiyama aldol addition to benzaldehyde. (b) Oxidative heteroarylation, synthesis of the α-pyrazole ketone derivative. (c) Three-step reaction, intramolecular substitution: synthesis of the tetrahydrofuran derivative.

other hand, the removal of the protecting group followed by the over-reduction of the ketone and ester groups, using an excess of NaBH$_4$, and the acid-mediated nucleophilic substitution (S$_N$1), resulted in the formation of the corresponding tetrahydrofuran derivative **9aa** in a 55% yield (Scheme 4c).

Mechanistic studies

Once we finished studying the scope, limitations and utility of the developed process, it was deemed appropriate to propose a mechanism based on literature reports and mechanistic studies. Our initial hypothesis involves a single electron transfer event that reduces **1a**, affording a radical intermediate that would yield the desired C–H functionalized or the cyclopropanation products, depending on the steric hindrance of the double bond. An alternative triplet sensitization process was dismissed because the reactions were carried out under air (see Scheme 5c). First, we conducted a study on different substitutions in the double bond, ranging from monosubstituted to disubstituted double bonds and silyl enol ethers under the standard photocatalytic conditions (Scheme 5a). Reactions with styrene derivatives (**4k–4n**) mainly afforded cyclopropanes, whereas the more hindered TBDMS-protected silyl enol ether (**2a**) or 1,1-diphenylethylene (**4a**) yielded the corresponding C–H functionalized products. In such cases, the ring-closing event to form the cyclopropane is unfavorable. That could be due to the steric hindrance afforded by the second substituent, favoring C–H functionalization that leads to the formation of Heck-type products (Scheme 5a and section 6.3 in the SI for all the tested double bonds). Next, we embarked on mechanistic studies such as the addition of a radical scavenger, luminescence quenching experiments, thermodynamic analysis and DFT calculations (Scheme 5b–c and 6b, and section 6.4 and 6.5 in the SI). To reveal the involvement of radical intermediates in the reaction pathway, the experiment was conducted in the presence of a radical-trapping agent such as butylated hydroxytoluene (BHT) or (2,2,6,6-tetra-

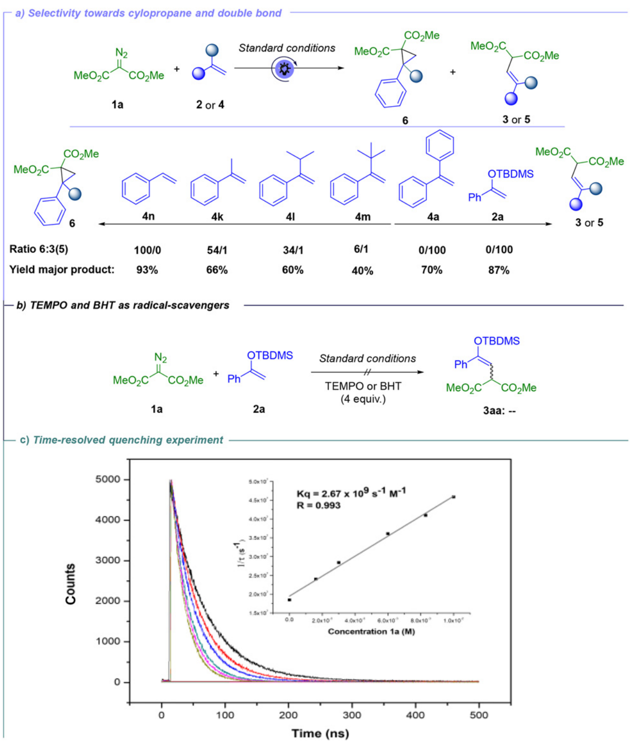

Scheme 5 Mechanistic studies. (a) Selectivity towards a cyclopropane or a double bond. (b) Reaction conducted with BHT or TEMPO as a radical scavenger. (c) Time-resolved luminescence quenching experiment of photoexcited *fac*-Ir(ppy)$_3$ in the presence of **1a** as a quencher.

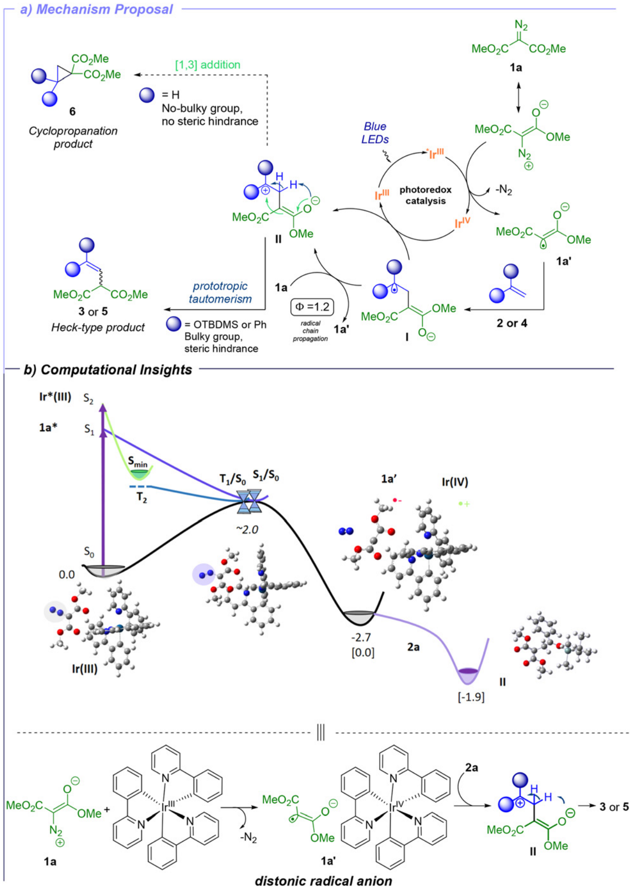

Scheme 6 Mechanistic proposal and DFT calculations. (a) Mechanistic proposal for the achievement of the photocatalytic Heck-type products (**3** and **5**) and the cyclopropanation product (**6**). (b) DFT and TD-DFT potential energy surfaces associated with the main mechanisms proposed here. Energies in eV are related to the Ir(III) ground state and in parentheses for the second step in the reaction.

methylpiperidin-1-yl)oxidanyl (TEMPO). In both cases, we found that the formation of **3aa** was observed in a very low amount (Scheme 5b), suggesting a single-electron transfer activation event. Moreover, the radical-trapped adduct with TEMPO was detected by EIS-HRMS analysis of the reaction crude (see Fig. S10 in the SI). These facts indicate that a single electron transfer activation event takes place. In addition, time-resolved luminescence quenching studies revealed an efficient interaction between the excited catalyst and **1a**, with a rate constant of $2.67 \times 10^9\ \mathrm{M}^{-1}\ \mathrm{s}^{-1}$, which indicates that **1a** quenches the luminescence emission of *fac*-Ir(ppy)$_3$ at a nearly diffusion-controlled rate (Scheme 5c and section 6.5 in the SI). Moreover, we also calculated the free energy change associated with electron transfer (ΔG_{ET}) from the excited state using the Rehm–Weller equation (eqn (1)).[20]

$$\Delta G_{\mathrm{ET}}\ (\mathrm{eV}) = [E_{\mathrm{ox}} - E_{\mathrm{red}} + (2.6/\varepsilon) - 0.13] - E*(\mathrm{T}_1) \tag{1}$$

Thus, considering that the values of the oxidation potential of the *fac*-Ir(ppy)$_3$ complex (E_{ox}), the reduction potential of **1a** (E_{red}), the excited state energy (E*(T$_1$)) and the dielectric constant (ε) of dichloromethane were 0.77 V *vs.* SCE,[21] −1.40 V *vs.* SCE, 2.50 eV[21] and 8.93 eV, respectively, we estimated a ΔG_{ET} value of −0.22 eV. Therefore, the primary electron transfer process from the luminescence emission of the excited photocatalyst is an exergonic process. On the other hand, there are no other reduction peak potentials related to **2a**, **4a** and **4k**, and their oxidation peak potentials are too positive (see section 6.1 in the SI); therefore, these species cannot quench the excited state of *fac*-Ir(ppy)$_3$. These results suggest that SET between the diazomalonate **1a** and the excited state of the photocatalyst is a key step of the photoredox cycle.

A plausible mechanism for the photocatalytic reaction is depicted in Scheme 6a. Under blue LED irradiation, the photoexcitation of the Ir(III) complex yields its photoexcited state Ir(III)* ($E_{1/2}^{\mathrm{IV/*III}} = -1.58$ V vs. SCE), which is oxidatively quenched by SET to the diazomalonate zwitterionic species **1a** ($E_{1/2}^{\mathrm{red}} = -1.40$ V *vs.* SCE) to produce Ir(IV) and the key distonic radical anion **1a′** of the malonate with the concomitant extrusion of N$_2$. Subsequent radical addition to the olefin partner yields the stabilized distonic benzylic radical anion **I**, which is further oxidized by Ir(IV), regenerating the ground state of *fac*-Ir(ppy)$_3$ and the zwitterionic carbocation intermediate **II.**

At this point, two possible pathways can be described depending on the steric hindrance of the groups in the olefin moiety. On the one hand (bold arrow), if bulky groups are subjected to photocatalytic conditions such as – OTBDMS or diaryl substituted ethylenes, a prototropic tautomerism takes place, which leads to the formation of Heck-type products (**3** or **5**). However, if the steric hindrance decreases, the formation of cyclopropanes is more favored (see Scheme 5a and section 6.3 in the SI), affording cyclopropanes as the sole products in reactions with styrene derivatives (dashed arrow). The cyclopropanation reaction takes place *via* direct addition of the nucleophilic carbon to the carbocation of intermediate **II** to yield the corresponding cyclopropane **6**. In addition, a high quantum yield (ø = 1.2) was determined, indicating a radical chain propagation, in which intermediate **I** can be oxidized by **1a**, thereby initiating the propagation process. As the formation of the intermediate distonic radical anion **1a′** is a key step, we decided to investigate its structure, stability, formation process, and the mechanism of electron transfer from Ir(III) to Ir(IV) using DFT and TD-DFT calculations with two different functionals (see section 8 in the SI).

Since iridium(IV) is cationic and species **1a′** is anionic, we also wondered about their possible interaction. The photoexcitation of the Ir(III) complex leads to the population of excited states whose nature has been characterized (Table S6). In detail, most of the lowest-lying excited states have some charge transfer character. Upon relaxation, the S$_1$ state reaches a crossing region with the ground state (S$_1$/S$_0$) through a barrierless path (Scheme 6b), where the N=N moiety significantly twists. Alternatively, S$_2$ optimization of Ir(III) leads to an emissive minimum (S$_{\mathrm{min}}$). At this region of the potential energy surface, the second triplet state (T$_2$) is degenerate in energy. We have characterized its evolution in the case of being populated and it directly reached a crossing region with the ground state (T_1/S_0), resembling the (S_1/S_0) state in energy and geometry. A potentially phosphorescent triplet minimum was also located when the Ir(III) complex was considered without the mediation of **1a** (see also section 8 in the SI for further evidence of the triplet character of the excited state).[22] Once in the S_0 state (from S_1/S_0 and/or T_1/S_0), the most stable situation leads to the formation of the Ir(IV) and **1a**′ species (Scheme 6b and Fig. S15 and S16), which exhibit an electrostatic interaction. In the next step, **1a**′ reacts with **2a** to form intermediate **II**, a process that proceeds without energy barriers, leading directly to the final product **3** or **5**.

Conclusions

In conclusion, a mild photocatalytic C(sp^2)–H functionalization of olefins using diazomalonates has been developed. The new synthetic strategy allows the functionalization of a wide variety of double bonds. The Heck-type products were obtained in overall very good yields, and further applications are demonstrated to highlight the utility of the process. This novel strategy, characterized by its mild conditions, is suitable for the late-stage functionalization of complex target molecules. The most plausible mechanism is based on the photocatalytic reduction of the diazo compound, followed by a reaction with the double bond to form the corresponding radical intermediate. After oxidation to the carbocation, the double bond is regenerated. The reaction pathway has been corroborated by electrochemical and photophysical experiments and computational studies.

Author contributions

M. A. V.-A., B. C., I. M., R. P.-R., L. M., A. F. and J. A. designed the experiments and analyzed the data. M. A. V.-A., B. C. and I. M. performed the experiments and prepared the SI. L. M.-F. performed the calculations and wrote the theoretical part of the article. L. M., A. F. and J. A. wrote the manuscript. All authors contributed to the discussion of the results. All authors have given approval to the final version of the manuscript.

Conflicts of interest

There are no conflicts to declare.

Data availability

The data supporting this article have been included as part of the supplementary information (SI). Supplementary information: experimental details, general procedures, optimization of reaction conditions, characterization of products, copies of NMR spectra of all products and mechanistic and computational details. See DOI: **https://doi.org/10.1039/d5qo01537e**.

Acknowledgements

Financial support was provided by the Spanish Government (PID2021-122299NB-I00, PID2008-146050NA-I00, PID2023-148367OB-I00, PID2023-146050NA-I00, TED2021-130470B-I00 and TED2021-129999B-C32), the 'Comunidad de Madrid', European Structural Funds (S2018/NMT-4367), and the proyectos sinérgicos I + D (Y2020/NMT6469). L. M. thanks the Ministerio de Ciencia e Innovación for a Ramón y Cajal contract (RYC2021-031590-I). I. M. thanks CAM for his fellowship (PIPF-2023/ECO-30898). This research project was made possible through the access granted by the Galician Supercomputing Center (CESGA) to its supercomputing infrastructure. The supercomputer FinisTerrae III and its permanent data storage system have been funded by the Spanish Ministry of Science and Innovation, the Galician Government and the European Regional Development Fund (ERDF).

References

1 (*a*) M. P. Doyle, M. A. McKervey and T. Ye, *Modern Catalytic Methods for Organic Synthesis with Diazo Compounds: from Cyclopropanes to Ylides*, John Wiley and Sons, 1998; (*b*) H. W. L. Davies and D. Morton, Guiding principles for site selective and stereoselective intermolecular C–H functionalization by donor/acceptor rhodium carbenes, *Chem. Soc. Rev.*, 2011, **40**, 1857–1869; (*c*) Ł. W. Ciszewski, K. Rybicka-Jasińska and D. Gryko, Recent development in photochemical reactions of diazo compounds, *Org. Biomol. Chem.*, 2019, **17**, 432–448.

2 (*a*) J. Fu, N. Wurzer, V. Lehner, O. Reiser and H. M. L. Davies, Rh(II)-Catalyzed Monocyclopropanation of Pyrroles and Its Application to the Synthesis Pharmaceutically Relevant Compounds, *Org. Lett.*, 2019, **21**, 6102–6106; (*b*) Y. Guo, C. Empel, C. Pei, I. Atodiresei, T. Fallon and R. M. Koenigs, Photochemical Cyclopropanation of Cyclooctatetraene and (Poly-)unsaturated Carbocycles, *Org. Lett.*, 2020, **22**, 5126–5130; (*c*) B. Morandi and E. M. Carreira, Iron-Catalyzed Cyclopropanation with Trifluoroethylamine Hydrochloride and Olefins in Aqueous Media: In Situ Generation of Trifluoromethyl Diazomethane, *Angew. Chem., Int. Ed.*, 2010, **49**, 938–941; (*d*) B. Morandi and E. M. Carreira, Iron-Catalyzed Cyclopropanation in 6 M KOH with in Situ Generation of Diazomethane, *Science*, 2012, **335**, 1471–1474; (*e*) D. H. Hodgson, F. Y. T. M. Pierard and P. A. Stupple, Catalytic enantioselective rearrangements and cycloadditions involving ylides from diazo compounds, *Chem. Soc. Rev.*, 2001, **30**, 50–61.

3 For selected reviews on rearrangement reactions, see: (*a*) S. Dong, X. Liu and X. Feng, Asymmetric Catalytic Rearrangements with α-Diazocarbonyl Compounds, *Acc. Chem. Res.*, 2022, **55**, 415–428; (*b*) S. Jana, Y. Guo and R. M. Koenigs, Recent Perspectives on Rearrangement Reactions of Ylides via Carbene Transfer Reactions, *Chem.*

– *Eur. J.*, 2021, **27**, 1270–1281; (*c*) H. Meier and K.-P. Zeller, The Wolff Rearrangement of α-Diazo Carbonyl Compounds, *Angew. Chem., Int. Ed. Engl.*, 1975, **14**, 32–43.

4 For selected reviews on insertion reactions, see: (*a*) M. P. Doyle, R. Duffy, M. Ratnikov and L. Zhou, Catalytic Carbene Insertion into C–H Bonds, *Chem. Rev.*, 2010, **110**, 704–724; (*b*) H. M. L. Davies and D. Morton, Guiding principles for site selective and stereoselective intermolecular C-H functionalization by donor/acceptor rhodium carbenes, *Chem. Soc. Rev.*, 2011, **40**, 1857–1869; (*c*) D. Gillingham and N. Fei, Catalytic X–H insertion reactions based on carbenoids, *Chem. Soc. Rev.*, 2013, **42**, 4918–4931.

5 D. M. Hodgson, F. Y. T. M. Pierard and P. A. Stupple, Catalytic enantioselective rearrangements and cycloadditions involving ylides from diazo compounds, *Chem. Soc. Rev.*, 2001, **30**, 50–61.

6 T. Xiao, M. Mei, Y. He and L. Zhou, Blue light-promoted cross-coupling of aryldiazoacetates and diazocarbonyl compounds, *Chem. Commun.*, 2018, **54**, 8865–8868.

7 (*a*) K. J. Hock, A. Knorrscheidt, R. Hommelsheim, J. Ho, M. J. Weissenborn and R. M. Koenigs, Tryptamine Synthesis by Iron Porphyrin Catalyzed C–H Functionalization of Indoles with Diazoacetonitrile, *Angew. Chem., Int. Ed.*, 2019, **58**, 3630–3634; (*b*) S. Jana, C. Empel, C. Pei, P. Aseeva, T. V. Nguyen and R. M. Koenigs, C–H Functionalization Reactions of Unprotected *N*-Heterocycles by Gold-Catalyzed Carbene Transfer, *ACS Catal.*, 2020, **10**, 9925–9931; (*c*) H. M. L. Davies and J. R. Mannig, Catalytic C–H functionalization by metal carbenoid and nitrenoid insertion, *Nature*, 2008, **451**, 417–424.

8 (*a*) *Contemporary Carbene Chemistry*, ed. R. A. Moss and M. P. Doyle, John Wiley & Sons, Inc., Hoboken, New Jersey, 2014; (*b*) Y. Xia, D. Qiu and J. Wang, Transition-Metal-Catalyzed Cross-Couplings through Carbene Migratory Insertion, *Chem. Rev.*, 2017, **117**, 13810–13889; (*c*) X. Guo and W. Hu, Novel Multicomponent Reactions via Trapping of Protic Onium Ylides with Electrophiles, *Acc. Chem. Res.*, 2013, **46**, 2427–2440; (*d*) S.-F. Zhu and Q.-L. Zhou, Transition-Metal-Catalyzed Enantioselective Heteroatom–Hydrogen Bond Insertion Reactions, *Acc. Chem. Res.*, 2012, **45**, 1365–1377.

9 (*a*) I. D. Jurberg and H. M. L. Davies, Blue light-promoted photolysis of aryldiazoacetates, *Chem. Sci.*, 2018, **9**, 5112–5118; (*b*) G. Cariello, R. D. C. Galloand, V. M. Deflon, R. A. Cormanich and I. D. Jurberg, Visible light-mediated formal alkylation and [4 + 1]-cycloaddition strategies of silyl enol ethers with aryldiazoacetates, *Chem. Commun.*, 2025, **61**, 2044–2047; see also: (*c*) T. Xiao, M. Mei, Y. He and L. Zhou, Blue light-promoted cross-coupling of aryldiazoacetates and diazocarbonyl compounds, *Chem. Commun.*, 2018, **54**, 8865–8868; (*d*) V. Klöpfer, R. Eckl, J. Floß, P. M. C. Roth, O. Reiser and J. P. Barham, *Green Chem.*, 2021, **23**, 6366–6372.

10 R. Hommelsheim, Y. Guo, Z. Yang, C. Empel and R. M. Koenigs, Blue-Light-Induced Carbene-Transfer Reactions of Diazoalkanes, *Angew. Chem., Int. Ed.*, 2019, **58**, 1203–1207.

11 (*a*) J. Durka, J. Turkowska and D. Gryko, Lightening Diazo Compounds?, *ACS Sustainable Chem. Eng.*, 2021, **9**, 8895–8918; (*b*) Z. Yang, M. Stivanin, I. D. Jurberg and R. M. Koenigs, Visible light-promoted reactions with diazo compounds: a mild and practical strategy towards free carbene intermediates, *Chem. Soc. Rev.*, 2020, **49**, 6833–6847.

12 (*a*) C. K. Prier, D. A. Rankic and D. W. C. MacMillan, Visible Light Photoredox Catalysis with Transition Metal Complexes: Applications in Organic Synthesis, *Chem. Rev.*, 2013, **113**, 5322–5363; (*b*) M. N. Hopkinson, B. Sahoo, J.-L. Li and F. Glorius, Dual Catalysis Sees the Light: Combining Photoredox with Organo-, Acid, and Transition-Metal Catalysis, *Chem. – Eur. J.*, 2014, **20**, 3874–3886; (*c*) J.-R. Chen, L.-Q. Lu and W.-J. Xiao, Visible light photoredox-controlled reactions of *N*-radicals and radical ions, *Chem. Soc. Rev.*, 2016, **45**, 2044–2056; (*d*) X. Lang, J. Zhao and X. Chen, Cooperative photoredox catalysis, *Chem. Soc. Rev.*, 2016, **45**, 3026–3038; (*e*) H. Huang, K. Jia and Y. Chen, Radical Decarboxylative Functionalizations Enabled by Dual Photoredox Catalysis, *ACS Catal.*, 2016, **6**, 4983–4988.

13 (*a*) F. Li, C. Pei and R. M. Koenigs, Photocatalytic gem-Difluoroolefination Reactions by a Formal C–C Coupling/Defluorination Reaction with Diazoacetates, *Angew. Chem., Int. Ed.*, 2022, **61**, e202111892; (*b*) C. Empel, S. Jana, Ł. W. Ciszewski, K. Zawada, C. Pei, D. Gryko and R. M. Koenigs, C–H Functionalization of Heterocycles with Triplet Carbenes by means of an Unexpected 1,2-Alkyl Radical Migration, *Chem. – Eur. J.*, 2023, **29**, e202300214.

14 M. Giedyk, K. Goliszewska, K. Proinsias and D. Gryko, Cobalt(I)-catalysed CH–alkylation of terminal olefins, and beyond, *Chem. Commun.*, 2016, **52**, 1389–1392.

15 (*a*) Y.-L. Su, G.-X. Liu, J.-W. Liu, L. Tram, H. Qiu and M. P. Doyle, Radical-Mediated Strategies for the Functionalization of Alkenes with Diazo Compounds, *J. Am. Chem. Soc.*, 2020, **142**, 13846–13855; (*b*) N. Ma, L. Guo, D. Qi, F. Gao, C. Yang and W. Xia, Visible-Light-Induced Multicomponent Synthesis of γ-Amino Esters with Diazo Compounds, *Org. Lett.*, 2021, **23**, 6278–6282; (*c*) Z. Zhang, N. Kvasovs, A. Dubrovina and V. Gevorgyan, Visible Light Induced Brønsted Acid Assisted Pd-Catalyzed Alkyl Heck Reaction of Diazo Compounds and *N*-Tosylhydrazones, *Angew. Chem., Int. Ed.*, 2022, **61**, e202110924.

16 (*a*) Ł. W. Ciszewski, J. Durka and D. Gryko, Photocatalytic Alkylation of Pyrroles and Indoles with α-Diazo Esters, *Org. Lett.*, 2019, **21**, 7028–7032; (*b*) W. Xu, Z. Zheng, G. Bao, Y. Wang, Y. Gao, H. Zhu, G. Xu, Y. Zhu, C. Yu and X. Jiang, Photocatalytic Three-Component Synthesis of 3-Heteroarylbicyclo[1.1.1]pentane-1-acetates, *Org. Lett.*, 2023, **25**, 4050–4055.

17 (*a*) A. C. Cope, H. L. Holmes and H. O. House, The Alkylation of Esters and Nitriles, *Org. React.*, 1957, **9**, 107–331; (*b*) R. J. Ouellette and J. D. Rawn, Condensation Reactions of Carbonyl Compounds, in *Organic Chemistry*

Structure, Mechanism, and Synthesis, Elsevier, 2nd edn, 2018, chapter 23, pp. 711–762.

18 (*a*) Z. Zhang and V. Gevorgyan, Visible Light-Induced Reactions of Diazo Compounds and Their Precursors, *Chem. Rev.*, 2024, **124**, 7214–7261; (*b*) M. Gao, C. Song, X. Liu, J. Zhao and P. Li, Photocatalytic Access to Cyclopropanes Via Triplet Carbene Transfer from Acceptor-Acceptor Diazoalkanes, *Org. Lett.*, 2026, **28**, 752–757.

19 (*a*) D. C. Magri and M. S. Workentin, A radical-anion chain mechanism following dissociative electron transfer reduction of the model prostaglandin endoperoxide, 1,4-diphenyl-2,3-dioxabicyclo[2.2.1]heptane, *Org. Biomol. Chem.*, 2008, **6**, 3354–3361; (*b*) K. Fu, X. Yang, Z. Yu, L. Song and L. Shi, Revealing the nature of covalently tethered distonic radical anions in the generation of heteroatom-centered radicals: evidence for the polarity-matching PCET pathway, *Chem. Sci.*, 2024, **15**, 12398–12409.

20 A. Weller, Photoinduced Electron Transfer in Solution: Exciplex and Radical Ion Pair Formation Free Enthalpies and their Solvent Dependence, *Z. Phys. Chem.*, 1982, **133**, 93–98.

21 K. A. King, P. J. Spellane and R. J. Watts, Excited-state properties of a triply ortho-metalated iridium(III) complex, *J. Am. Chem. Soc.*, 1985, **107**, 1431–1432.

22 (*a*) K.-C. Tang, K. L. Liu and I.-C. Chen, Rapid intersystem crossing in highly phosphorescent iridium complexes, *Chem. Phys. Lett.*, 2004, **386**, 437–441; (*b*) J. Li, P. I. Djurovich, B. D. Alleyne, M. Yousufuddin, N. N. Ho, J. C. Thomas, J. C. Peters, R. Bau and M. E. Thompson, Synthetic Control of Excited-State Properties in Cyclometalated Ir(III) Complexes Using Ancillary Ligands, *Inorg. Chem.*, 2005, **44**, 1713–1727; (*c*) G. J. Hedley, A. Ruseckas and I. D. W. Samuel, Ultrafast luminescence in Ir(ppy)$_3$, *Chem. Phys. Lett.*, 2008, **450**, 292–296; (*d*) J.-H. Kim, S.-Y. Kim, D. W. Cho, H.-J. Son and S. O. Kang, Influence of bulky substituents on the photophysical properties of homoleptic iridium(III) complexes, *Phys. Chem. Chem. Phys.*, 2019, **21**, 6908–6916.